

1 Understanding adsorption of hydrogen atoms on graphene

2 Simone Casolo,^{1,a)} Ole Martin Løvrik,^{1,2} Rocco Martinazzo,^{3,b)} and
 3 Gian Franco Tantardini^{3,4}

4 ¹Department of Physics, University of Oslo, P.O. Box 1048 Blindern, NO-0316 Oslo, Norway

5 ²SINTEF Materials and Chemistry, Forskningsvn 1, NO-0314 Oslo, Norway

6 ³Department of Physical Chemistry and Electrochemistry and CIMAINA, University of Milan,
 7 V. Golgi 19, 20133 Milan, Italy

8 ⁴Institute for Molecular Science and Technology (ISTM), V. Golgi 19, 20133 Milan, Italy

9 (Received 1 October 2008; accepted 22 December 2008; published online xx xx xxxx)

10 Adsorption of hydrogen atoms on a single graphite sheet (graphene) has been investigated by
 11 first-principles electronic structure means, employing plane-wave based periodic density functional
 12 theory. A 5×5 surface unit cell has been employed to study single and multiple adsorptions of H
 13 atoms. Binding and barrier energies for sequential sticking have been computed for a number of
 14 configurations involving adsorption on top of carbon atoms. We find that binding energies per atom
 15 range from ~ 0.8 to ~ 1.9 eV, with barriers to sticking in the range 0.0–0.15 eV. In addition,
 16 depending on the number and location of adsorbed hydrogen atoms, we find that magnetic structures
 17 may form in which spin density localizes on a $\sqrt{3} \times \sqrt{3}R30^\circ$ sublattice and that binding (barrier)
 18 energies for sequential adsorption increase (decrease) linearly with the site-integrated
 19 magnetization. These results can be rationalized with the help of the valence-bond resonance theory
 20 of planar π conjugated systems and suggest that preferential sticking due to barrierless adsorption
 21 is limited to formation of hydrogen pairs. © 2009 American Institute of Physics.

22 [DOI: 10.1063/1.3072333]

23

24 I. INTRODUCTION

25 Recent years have witnessed an ever growing interest in
 26 carbon-based materials. Carbon, being a small atom with a
 27 half-filled shell, is able to mix its valence s and p orbitals to
 28 various degrees, thereby forming the building block for ex-
 29 tended structures of incredibly different electronic, magnetic,
 30 and mechanical properties. Among them, those formed by
 31 sp^2 C atoms have attracted much attention in the past few
 32 years. They can be collectively termed as graphitic com-
 33 pounds and comprise graphite, carbon nanotubes, fullerenes,
 34 polycyclic aromatic hydrocarbons (PAHs), and recently
 35 graphene (the one-atom thick layer of graphite) and graphene
 36 nanoribbons (GNRs). In particular, the revolutionary (and
 37 embarrassing simple) fabrication of graphene¹ has opened
 38 the way for a wealth of studies in both fundamental and
 39 applied science. New extraordinary properties have become
 40 available to material design since its isolation. Indeed, even
 41 though they have been known since the first theoretical
 42 analysis by Wallace,² it was only the experimental observa-
 43 tion of the existence of the one-atom thick layer of graphite
 44 that triggered much of the current interest. In particular, one
 45 of the most interesting aspects of graphene is that it presents
 46 low energy excitations as massless, chiral, Dirac fermions
 47 mimicking the physics of quantum electrodynamics.^{3–5}

48 In this context, adsorption of hydrogen atoms on
 49 graphene and GNRs can be used to tailor electronic and mag-
 50 netic properties, as already suggested for other “defects,”

with the advantage of being much easier to realize than, e.g.,
 vacancies. In addition, interaction of hydrogen atoms with
 graphitic compounds has been playing an important role in a
 number of fields as diverse as nuclear fusion,^{6,7} hydrogen
 storage,⁸ and interstellar chemistry.⁹

In material design for hydrogen storage, several carbon-
 based structures have been proposed as candidates,⁸ in par-
 ticular, in connection with the spillover effect following em-
 bedding of metallic nanoparticles. Though these materials
 are in practice still far from the wt % target stated by the
 U.S. Department of Energy, they remain a cheap and safe
 alternative, and a deeper understanding of the mechanisms
 underlying adsorption may lead in future to a more efficient
 material design.

In interstellar chemistry hydrogen-graphite and
 hydrogen-PAH systems have become realistic models to in-
 vestigate molecular hydrogen formation in the interstellar
 medium (ISM). There are still open questions in this context
 since, in spite of continuous destruction by UV radiation and
 cosmic rays, H₂ is the most abundant molecule of the ISM. It
 is now widely accepted that H₂ can only form on the surface
 of interstellar dust grains and particles,^{10–12} which—with the
 exception of cold dense molecular clouds—are either
 carbon-coated silicate grains or carbonaceous particles or
 large PAHs.^{13–15} This finding has stimulated a number of
 theoretical^{16–33} and experimental^{19,34–43} studies on hydrogen
 graphitic systems aimed at elucidating the possible reaction
 pathways leading ultimately to molecule formation.

One interesting finding of these studies is the tendency
 of hydrogen atoms to cluster at all but very low coverage
 conditions.^{37–39,43} New mechanisms for hydrogen

^{a)}On leave from Department of Physical Chemistry and Electrochemistry,
 University of Milan.

^{b)}Electronic mail: rocco.martinazzo@unimi.it.

82 sticking^{25,39} and new recombination pathways³⁸ have been
 83 proposed, based on the now common agreement that the
 84 presence of one or more adsorbate atoms strongly influences
 85 subsequent adsorption. It is clear that such an influence can
 86 only result as a consequence of a substrate-mediated interac-
 87 tion which makes use of the unusual electronic properties of
 88 graphitic compounds, but at present a comprehensive model
 89 for multiple chemisorptions is still missing.

90 In this work we present first-principles calculations of
 91 single and multiple adsorptions of hydrogen atoms on a
 92 graphene sheet, used as a model graphitic material, with the
 93 aim of understanding the relationship between the substrate
 94 electronic properties and the stability of various cluster con-
 95 figurations. This work parallels analogous investigations of
 96 defects in graphene and GNRs.^{44–49} Indeed, they all share the
 97 disappearance of one or more carbon p orbitals from the
 98 π - π^* band system, a fact which may lead to the appearance
 99 of magnetic textures and introduce site-specific dependence
 100 on the chemical properties. Complementing previous inves-
 101 tigation, however, we show how the simple π resonance
 102 chemical model helps in rationalizing the findings. A parallel
 103 work on different graphitic substrates (PAHs) will follow
 104 shortly.⁵⁰

105 This paper is organized as follows. Details of our first-
 106 principles calculations are given in Sec. II, and their results
 107 in Sec. III, where we analyze adsorption of a single H atom
 108 and briefly introduce the chemical picture (Sec. III A), we
 109 consider formation of pairs (Sec. III B) and formation of
 110 three- and four-atom clusters (Sec. III C). We summarize and
 111 conclude in Sec. IV.

112 II. COMPUTATIONAL METHODS

113 Periodic density functional theory (DFT) as imple-
 114 mented in the Vienna *ab initio* simulation package suite
 115 (VASP)^{51–54} has been used in all the calculations. The
 116 projector-augmented wave method within the frozen core ap-
 117 proximation has been used to describe the electron-core
 118 interaction,^{55,56} with a Perdew–Burke–Ernzerhof^{57,58} func-
 119 tional within the generalized gradient approximation. Due to
 120 the crucial role that spin plays in this system all our calcula-
 121 tions have been performed in a spin unrestricted framework.
 122 All calculations have used an energy cutoff of 500 eV
 123 and a $6 \times 6 \times 1$ Γ -centered k -point mesh to span the electron
 124 density, in a way to include all the special points of the cell.
 125 The linear tetrahedron method with Blöchl corrections is
 126 used⁵⁹ together with a 0.2 eV smearing. All the atomic posi-
 127 tions have been fully relaxed until the Hellmann–Feynman
 128 forces dropped below 10^{-2} eV \AA^{-1} , while convergence of
 129 the electronic structures has been ensured by forcing the en-
 130 ergy difference in the self-consistent cycle to be below
 131 10^{-6} eV. In order to compute energy barriers the electronic
 132 temperature parameter has been decreased to 0.05 eV, and
 133 electronic solutions have been carefully checked to represent
 134 the correct spin-polarized ones needed to describe bond-
 135 breaking/bond-forming processes.

136 The slab supercell considered has been carefully tested
 137 and a 20 \AA vacuum along the c axis has been adopted to
 138 ensure no reciprocal interaction between periodical images.

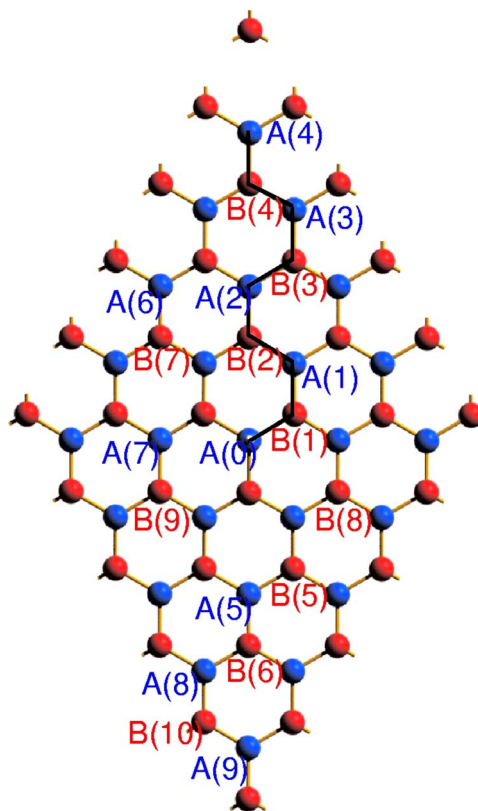


FIG. 1. (Color online) The graphene unit cell used for the calculations with A (blue) and B (red) lattice sites indicated. Also indicated is the path used for Fig. 3, A(0) being the first H adsorption site.

AQ:
#17

We find that by using the above settings the interaction be-
 139 tween two adjacent graphite layers is ~ 2 meV, largely
 140 within the intrinsic DFT error. This result is in agreement
 141 with literature data.^{60,61} For this reason a single graphene
 142 sheet can also model the Bernal (0001) graphite surface, at
 143 least as long as chemical interactions are of concern.
 144

The cell size on the surface plane is a fundamental pa-
 145 rameter for these calculations since we have found that
 146 chemisorption energies strongly depend on the coverage (see
 147 below). We choose to use a relatively large 5×5 cell in order
 148 to get some tens of meV accuracy while keeping the compu-
 149 tational cost as low as possible. Even with this size, however,
 150 the possibility of interactions between images has always to
 151 be taken into account when rationalizing the data.
 152

The cell used in this work is shown in Fig. 1, along with
 153 a labeling system for a number of lattice sites. Note that the
 154 graphene lattice consists of two equivalent sublattices (here
 155 and in the following denoted as A and B) which may become
 156 no longer equivalent upon H adsorption.
 157

158 III. RESULTS

159 A. Single atom adsorption

Chemisorption of single H atoms on graphite has long
 160 been studied since the works of Jeloaica and Sidis¹⁶ and Sha
 161 and Jackson,¹⁷ who first predicted surface reconstruction
 162 upon sticking. Such a reconstruction, i.e., the puckering of
 163 the carbon atom beneath the adsorbed hydrogen atom, occurs
 164 as a consequence of sp^2 - sp^3 rehybridization of the valence
 165

TABLE I. Chemisorption energy (E_{chem}) and equilibrium height of the C atom above the surface (d_{puck}) for H adsorption on top of a C atom, for a number of surface unit cells, corresponding to different coverages θ .

Unit cell	θ (ML)	d_{puck} (Å)		E_{chem} (eV)	
		This work	Others	This work	Others
2×2	0.125	0.36	0.36 ^a	0.75	0.67 ^a
3×3	0.062	0.42	0.41 ^b	0.77	0.76 ^b
Cluster	0.045	...	0.57 ^c	...	0.76 ^c
4×4	0.031	0.48	...	0.79	0.76, ^d 0.85 ^c
5×5	0.020	0.59	...	0.84	0.71, ^f 0.82 ^g
8×8	0.008	0.87 ^h

^aReference 17.

^bReference 62.

^cReference 63.

^dReference 64.

^eReference 39.

^fReference 65.

^gReference 66.

^hReference 67.

166 C orbitals needed to form the σ CH bond. Since this
167 electronic/nuclear rearrangement causes the appearance of an
168 energy barrier ~ 0.2 eV high, sticking of hydrogen atoms
169 turns out to be a thermally activated process which hardly
170 occurs at and below room temperature.⁶²

171 As already said in Sec. II, we have reconsidered adsorp-
172 tion of single hydrogen atoms for different sizes of the sur-
173 face unit cell. We have found that both the binding energy
174 and the puckering height are strongly affected by the size of
175 the unit cell (see Table I), and even the results of the 5×5
176 cell turn out to be in error of about ~ 30 meV with respect to
177 the isolated atom limit estimated by the calculation at 0.008
178 ML coverage.⁶⁷ In particular, we have found that some cau-
179 tion is needed when comparing the height of the carbon atom
180 involved in the bond since constraining the neighboring car-
181 bon atoms in geometry optimization may lead to consider-
182 able surface strain.

183 Despite this, we have consistently used the 5×5 cell in
184 studying multiple adsorptions of hydrogen atoms. Indeed,
185 this size allowed us to investigate a number of stable con-
186 figurations involving two, three, and four adsorbed H atoms,
187 along with the barrier to their formation, with the same setup
188 described in Sec. II. Interactions between images do indeed
189 occur for some configurations but, as we show below, this
190 does not prevent us to get a clear picture of the adsorption
191 processes we are interested in.

192 In agreement with previous studies we find that hydro-
193 gen adsorption can only occur if the substrate is allowed to
194 relax. Without relaxation the adsorption curves on different
195 surface sites are repulsive, and only a metastable minimum is
196 found for the atop position.¹⁷ Surface relaxation requires
197 about 0.8–0.9 eV (this is the energy needed to pucker the
198 free graphene sheet as required by adsorbing one H atom on
199 top of a carbon atom) and results in the outward motion of
200 the carbon atom forming the CH bond (see Table I and Refs.
201 16 and 17). We note that the results of Boukhvalov *et al.*⁶⁸
202 are at variance with a number of literature data (see, e.g.,
203 Table I and reference therein, compared with Table I of Ref.
204 68). Special care was therefore devoted to try to reproduce
205 their energetic and geometrical results, without any success.

We carefully checked our convergence of electronic and geo- 206
metrical optimizations, and Sec. II should give enough de- 207
tails to guarantee data reproducibility. 208

In addition, we have investigated the electronic substrate 209
properties of the resulting hydrogenated graphene, in order to 210
get hints for understanding the adsorption process of addi- 211
tional atoms. In Fig. 2 we show the density of states (DOS) 212
of the 5×5 H-graphene equilibrium structure (bottom 213
panel), compared to that of clean graphene (top panel). It is 214
evident from the figure that hydrogen adsorption causes the 215
appearance of a double peak in the DOS, symmetrically 216
placed around the Fermi level. This is in agreement with 217
rigorous results that can be obtained in tight-binding theory 218
for *bipartite* lattices. Indeed, Inui *et al.*⁶⁹ showed that for a 219
bipartite lattice with n_A A lattice sites and n_B B lattice sites a 220
sufficient condition for the existence of midgap states is a 221
lattice imbalance ($n_A \neq n_B$). In particular, there exist $n_I = |n_A$ 222
 $- n_B|$ midgap states with *vanishing* wavefunction on the mi- 223
nority lattice sites. In H graphene a lattice imbalance results 224

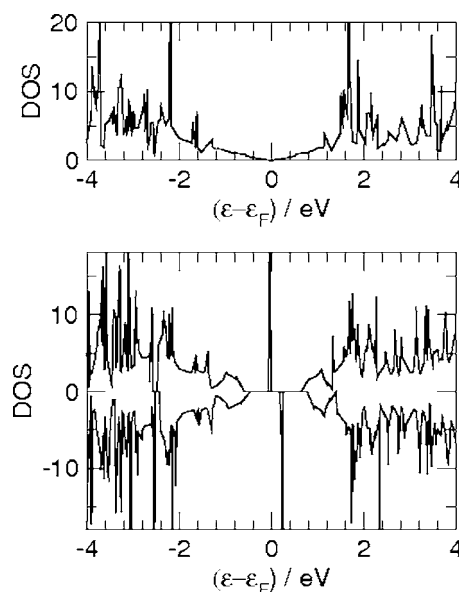


FIG. 2. Top panel: total DOS for graphene; Bottom panel: DOS for spin-up (positive values) and spin-down (negative values) components in a 5×5 H layer on graphene.

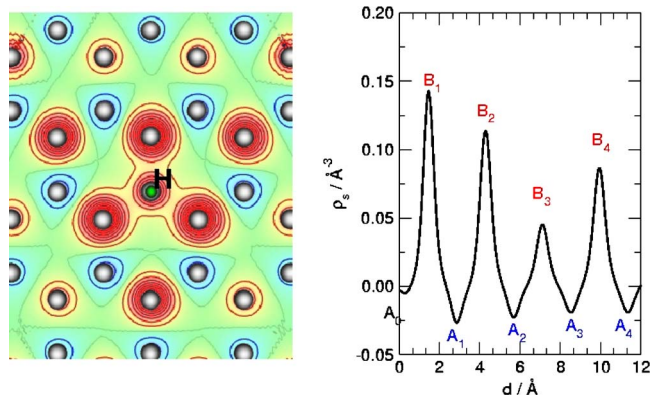


FIG. 3. (Color online) Spin density of 0.47 Å above the graphene surface after adsorption of a hydrogen atom. Left: contour map with red/blue lines for spin-up/spin-down excess, respectively. Right: spin density at the same height as on the left panel, along a path joining the C atoms (for the labels see Fig. 1).

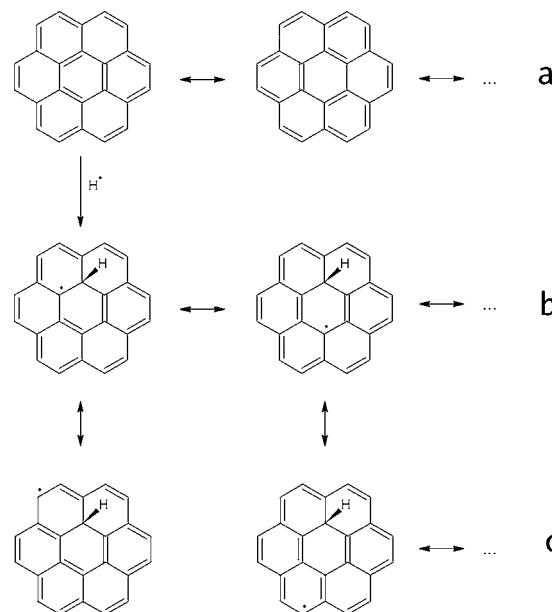


FIG. 4. (a) The π resonating chemical model for a graphenic surrogate (coronene). [(b) and (c)] Spin alternation after hydrogen adsorption.

225 as a consequence of the bond with the H atom which makes
 226 one of p orbitals no longer available for taking part to the
 227 π - π^* band system. There is one midgap state for each spin
 228 species, and the degeneracy is lifted if exchange-correlation
 229 effects are taken into account, as shown in Fig. 2 for our
 230 DFT results. This state has been mapped out in Fig. 3 (left
 231 panel), where we report a contour map of the spin density at
 232 a constant height of 0.47 Å above the surface. It is clear from
 233 the figure that if adsorption occurs on an A lattice site the
 234 spin density (due mainly to the above midgap state) localizes
 235 on B lattice sites. The latter now contain most of the $1\mu_B$
 236 magnetization (μ_B denotes Bohr magneton) previously car-
 237 ried by the H atom species, and a slight spin-down excess on
 238 A sites results as a consequence of the spin polarization of
 239 the lower-lying states. This is made clearer in the right panel
 240 of Fig. 3 where we report the spin density at the same height
 241 above the surface as before along a rectilinear path joining a
 242 number of C atom sites away from the adsorption site (see
 243 Fig. 1 for the labels). Note that the spin density decays only
 244 slowly with the distance from the adsorption site, in agree-
 245 ment with theoretical results that suggest that in the case of
 246 two dimensional graphene this decay corresponds to a non-
 247 normalizable state with a $1/r$ tail (in contrast to nonzero gap
 248 substrates such as armchair nanoribbons where midgap states
 249 are normalizable).⁴⁴ With our unit cell the effect of the inter-
 250 action with the images is already evident at rather short dis-
 251 tances, but as we show below, this effect has no influence on
 252 the interpretation of the results. Note also that this spin pat-
 253 tern is common to other defects (e.g., vacancies, voids, and
 254 edges) which have been known for some time to strongly
 255 modify the electronic properties of graphene and graphene-
 256 like structures and to (possibly) produce long-range ordered
 257 magnetic structures.^{44–49,67,70–75} In particular, in a recent
 258 comprehensive study Palacios *et al.*,⁴⁸ using a mean-field
 259 Hubbard model for graphene, clarified the appearance of
 260 magnetic textures associated with vacancies and predicted
 261 the emergence of magnetic order. Their model also suits well
 262 to defects such as the presence of the adsorbed hydrogen
 263 atoms.

known “spin alternation” typical of π conjugated com-
 266 pounds. This behavior is easily understood in terms of reso-
 267 nant chemical structures, such as those shown in Fig. 4 for a
 268 coronene molecule. In this and analogous PAHs, the π elec-
 269 tron system can be described as a combination of conven-
 270 tional alternated double bond structures, like the ones shown
 271 in Fig. 4 (see a). Once a hydrogen atom has been adsorbed
 272 on the surface, an unpaired electron is left on one of the
 273 neighboring C atoms (b, left panel), which can subsequently
 274 move in each of the carbon atoms belonging to a sublattice
 275 $\sqrt{3} \times \sqrt{3}R30^\circ$ by “bond switching” (see b and c). Spin alter-
 276 nation arises from the “resonant” behavior of an unpaired
 277 electron in α position (the nearest neighbor one) with respect
 278 to a double bond: such “resonance” can be naively viewed as
 279 the spin recoupling of the unpaired electron with the
 280 electron on the neighboring site, a process which sets free a second
 281 electron on the same sublattice.
 282

It is worth noticing at this point that this simple picture
 283 has solid roots in quantum mechanics, namely, in the valence
 284 bond (VB) theory of chemical bonding.⁷⁶ This theory was
 285 formulated soon after the advent of quantum mechanics by
 286 Heitler and London⁷⁷ and Pauling and Slater, and initially
 287 aimed at rationalizing successful prequantum ideas about
 288 bonding in molecules, such as the Lewis structures and the
 289 octet rule. Since the beginning, it correctly described bond-
 290 forming and bond-breaking processes and spin-recoupling
 291 and hybridization phenomena and provided rigorous justifi-
 292 cation of concepts such as structures and resonance between
 293 structures. Later, it developed as an *ab initio* approach,^{78,79}
 294 complementary to molecular orbital (MO) based electronic
 295 structure theories, with the disadvantage of using nonor-
 296 thogonal many-electron basis but the advantage of providing
 297 a clear picture of electronic structures.
 298

For a π electron system, a simple (correlated) VB *ansatz*
 299 for the N electron wavefunction of the π cloud reads as
 300

AQ:
 #1

AQ:
 #2

AQ:
 #3

AQ:
 #4

AQ:
 #5

$$\Psi_{SN} = \mathcal{A}(\phi_1 \phi_2 \cdots \phi_N \Theta_{SN}), \quad (1)$$

AQ: #6 302 where \mathcal{A} is the antisymmetric projector, $\phi_i = \phi_i(\mathbf{r})$ for i
 303 $= 1, N$ are (spatial) orbitals accommodating the N electrons,
 304 and Θ_{SN} is an N electron spin function with spin quantum
 305 number S . The latter is usually variationally optimized by
 306 expansion on a spin basis $\{\Theta_{SN;k}\}_{k=1, f_S^N}$ of \mathbf{S}^2 eigenvectors
 307 with eigenvalue $S(S+1)$ (and given magnetization). Chemi-
 308 cal ideas are brought into the theory by using the “perfect
 309 pairing” spin basis devised by Rumer⁸⁰ in which, for a given
 310 S and $M_s = S$, the total magnetization is given by $2S$ electrons
 311 coupled at high spin, the remaining $N - 2S$ being accommo-
 312 dated in $(N - 2S)/2$ singlet-coupled pairs. Indeed, if the or-
 313 bitals ϕ_i are *localized* on the atoms, the resulting wavefunc-
 314 tion

$$\Psi_{SN} = \sum_{k=1, f_S^N} c_k \mathcal{A}(\phi_1 \phi_2 \cdots \phi_N \Theta_{SN;k}) = \sum_{k=1, f_S^N} c_k \Psi_{SN;k}$$

315 is a superposition of conventional “structures” $\Psi_{SN;k}$ describ-
 316 ing pairs of atom-centered singlet-coupled orbitals (i.e.,
 317 Lewis chemical bonds and lone pairs) and unpaired elec-
 318 trons. Simple molecules require just one perfect-pairing spin
 319 function coupling those pairs of orbitals with substantial
 320 overlap. Less conventional molecules, such as π conjugated
 321 systems, need a true superposition of two or more spin struc-
 322 tures since the energy gain (the *resonance* energy) in allow-
 323 ing such superposition is sizable in these cases. Correspond-
 324 ingly, the classical Lewis picture of chemical bonds is
 325 extended to account for the resonance phenomenon, as
 326 shown in Fig. 4 with double ended arrows indicating *super-*
 327 *position* of chemical structures.

329 Early applications of the VB theory used frozen atomic
 330 orbitals, whereas nowadays^{81–84} both the spin-coupling coef-
 331 ficients c_k and the orbitals can be variationally optimized,
 332 even when using a number of configurations in place of the
 333 single-orbital product appearing in Eq. (1). The interesting
 334 thing is that these optimized orbitals, as a consequence of
 335 electron correlation, are usually (if not always) localized on
 336 atomic centers and are only slightly polarized by the envi-
 337 ronment, thereby supporting the interpretation of the simple
 338 wavefunction of Eq. (1) as a quantum-mechanical translation
 339 of Lewis theory of chemical bond. This is true, in particular,
 340 for the benzene molecule, the prototypical π resonant sys-
 341 tem, where six p -like orbitals are mostly coupled by two
 342 so-called Kekulé structures.^{85–87} (For $S=0$ and $N=6$ the set
 343 of five linearly independent Rumer structures of the benzene
 344 π system is given by two Kekulé structures and the three
 345 additional “Dewar” structures. With orbital optimization, a
 346 resonance energy ≈ 0.8 eV can be computed when using two
 347 Kekulé structures in place of one, whereas only some tenths
 348 of meV are gained when full optimization of the spin func-
 349 tion is performed.⁵⁰)

350 From a physical point of view, wavefunction (1) can be
 351 considered a generalization to N electron systems of the
 352 Heitler–London ansatz forming the basis for the Heisenberg
 353 model of magnetism in insulators. In addition, if the orbitals
 354 are allowed to be “polarized,” bandlike behavior can be ac-
 355 commodated along with collective spin excitations, as in the
 356 Hubbard model⁸⁸ which has been finding widespread use in

investigating graphitic compounds. The fact that Hubbard 357
 model, and its Heisenberg limit, can be derived by suitable 358
 approximations to VB ansatz has long been known in the 359
 chemical literature, especially in connection to π resonant 360
 systems (see, e.g., Refs. 89 and 90 and references therein. 361
 Hubbard model is also known as Pariser–Parr–Pople model, 362
 after Pariser and Parr^{91,92} and after Pople⁹³). We can roughly 363
 say that Heisenberg models correspond to the “classical” va- 364
 lence theory using orbitals constrained to have their free- 365
 atom form, whereas Hubbard models arise by allowing them 366
 to be deformed by the chemical environment. 367

In Secs. III B and III C, we will use wavefunction of Eq. 368
 (1) as a simple guide to interpret the results of our first- 369
 principles calculations, keeping in mind its connections with 370
 the traditional chemical picture on the one hand and the Hub- 371
 bard model on the other hand. As we will show in the fol- 372
 lowing, even at this qualitative level, a number of useful 373
 insights can be gained from such a picture. 374

It is worth noticing at this point that these “VB consid- 375
 erations” do not rely on the existence of any symmetry in the 376
 system and therefore apply equally well to symmetric and 377
 nonsymmetric systems (like the defective structures consid- 378
 ered in Secs. III B and III C or finite-size systems such as 379
 PAHs). Symmetry, if present, is best exploited in single- 380
 particle theories when single-particle states are eigenfunc- 381
 tions of symmetric effective one-particle Hamiltonians, and 382
 indeed notable work has been done on graphene and GNRs 383
 with tight-binding Hamiltonians (see, e.g., Ref. 94 for a com- 384
 prehensive overview). [Note that in the ansatz of Eq. (1)— 385
 which has its origin in the separated atom limit—spatial 386
 symmetry is inextricably linked to spin space.] Even in these 387
 cases, however, correct description of magnetic ordering and 388
 related effects on band structures (see, e.g., Ref. 95) needs 389
 many-particle theories. The same is true for the bond- 390
 breaking/bond-forming processes considered here which, 391
 strictly speaking, cannot be handled with single-particle 392
 theories because of the well-known static correlation prob- 393
 lem. 394

As a first example we can reconsider adsorption of a 395
 single hydrogen atom on graphene. In a diabatic picture (i.e., 396
 when constraining the spin coupling to the Kekulé structures 397
 of Fig. 4, panel a) the interaction between graphene and the 398
 incoming H atom is expected to be repulsive since no elec- 399
 tron is available to form the CH bond. On the other hand, a 400
 low-lying spin-excited state corresponding to a Dewar-like 401
 structure (which has two singlet-paired electrons on oppo- 402
 site, no-overlapping end of a benzene ring) would give rise 403
 to an attractive barrierless interaction. At short range, then, 404
 an avoided crossing between the two doublet curves occurs 405
 which signals the spin transition leading to bond formation, 406
 even though this can lead only to a metastable state if surface 407
 reconstruction is not allowed, as indeed found in DFT calcu- 408
 lations (e.g., see Fig. 2 in Ref. 17). Actually, in this case the 409
 situation is a bit more complicated since a slightly lower- 410
 lying state in the triplet manifold (obtained by spin flipping 411
 the above spin-excited Dewar-like structure) contributes to 412
 the same doublet manifold. VB calculations on the simpler 413
 H-benzene system confirm this picture,⁵⁰ see Fig. 5. [Single- 414
 point VB calculations have been performed with the help of 415

AQ:
#7

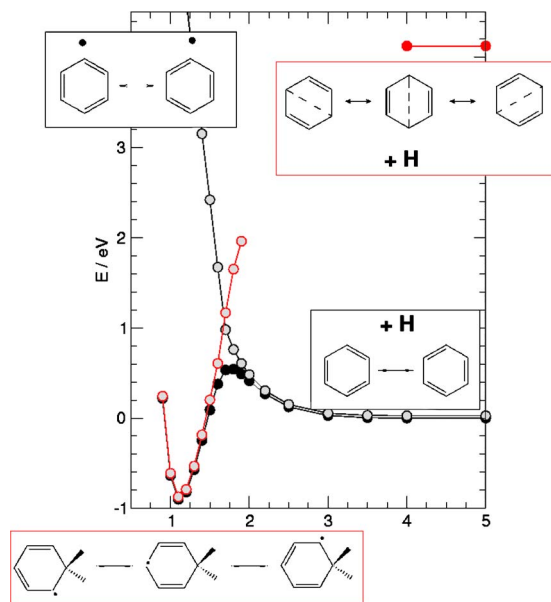


FIG. 5. (Color online) Interpretation of the sticking barrier as an avoided crossing between chemical structures. VB results for the benzene-H system, from Ref. 50. Solid black and red circles for the ground [$C_6H_6(^1A_{1g}) + H(^2S)$] and the first excited states [$C_6H_6(^3B_{1u}) + H(^2S)$], as obtained at the single-orbital-string level of Eq. (1), with orbital optimization. Quasidiabatic results are obtained by properly constraining the spin space. Kelulè structures only (lower right and upper left insets) for empty black circles; structures in the lower left inset for empty red circles. Also shown in the upper right inset are the main (Dewar-like) structures needed to describe the $^3B_{1u}$ state of benzene.

TABLE II. Binding energies (E_{bind}) for secondary adsorption to form the H pairs shown in Fig. 1, along with the site-integrated magnetizations (M_{SI}) before adsorption and the total ground-state magnetization (M) after adsorption obtained when fully relaxing the magnetization. Also reported are the binding energies obtained when the magnetization is constrained to $M = 0, 2\mu_B$ for A and B sites, respectively. See text for details.

Position	M_{SI} (μ_B)	E_{bind} (eV)	M (μ_B)	E_{bind}^* (eV)
B(1)	0.109	1.934	0	0.933
A(1)	-0.019	0.802	2	0.575
B(2)	0.085	1.894	0	0.828
A(2)	-0.017	0.749	2	0.531
B(3)	0.040	1.338	0	0.646
A(3)	-0.016	0.747	2	0.570
B(4)	0.076	1.674	0	...
A(4)	-0.016	0.747	2	0.573
B(5)	0.023	1.033	0	0.590
A(5)	-0.014	0.749	2	0.531
B(6)	0.028	1.110	0	0.545
A(6)	-0.015	0.787	2	...

been obtained by integrating the spin density on a small cylinder (of radius half of the C-C distance in the lattice) centered on each site and can be considered a rough measure of the total spin excess available on the site. This quantity behaves very similar to the spin density itself, decreasing in magnitude when increasing the distance from the adsorption site, *separately* for each sublattice. Some exceptions are worth noticing, namely, the A(0)-B(4) pair, and are due to the cumulative effect of next-neighbor images. Notice, however, that despite their possible artificial nature, results corresponding to any lattice sites when viewed as a function of the site-integrated magnetization give insights into the adsorption process.

A quick look at Table II reveals that the two sublattices A and B behave very different from each other, as the spin-coupling picture of Fig. 4 (panels b and c) suggests. Roughly speaking, adsorption on the B lattice is preferred over that on the A lattice. The binding energies are much larger than the first adsorption energy reported in Table I (they can be as large as twice the adsorption of the first atom) and give rise to a final unmagnetized state. In contrast, the binding energy for adsorption on the A lattice site is comparable to that of single H adsorption, and the ground state of the H pair on graphene is a triplet ($M=2\mu_B$).

These findings agree with Lieb's theorem¹⁰⁰ for the repulsive Hubbard model of a bipartite lattice and a half-filled band, which states that the ground state of the system has $S=1/2|n_A-n_B|$. In such model, the electronic state of the system would be described by $N-2$ p orbitals (N being the original number of sites), and $n_B=n_A=N/2-1$ if adsorption of the second hydrogen atom proceeds on the B lattice (to form what we can call AB dimers), whereas $n_B=n_A+2=N/2$ if it proceeds on the A lattice (to form A_2 dimers). The results are also consistent with the VB framework sketched in Sec. III A: with reference to Fig. 4 (panels b and c), it is clear that when a H atom adsorbs on a B site its electron readily couples with the unpaired electron available on the B sublattice, whereas when adsorption occurs on an A site two

the VB2000 code^{96,84} on the geometries optimized at the DFT-UB3LYP level, as implemented in the GAMESS code,⁹⁷ using in both cases the cc-pVDZ atom-centered basis set. Two group functions⁹⁸ have been defined and simultaneously optimized: a VB group containing nine electrons in nine orbitals [Eq. (1)] and a Hartree-Fock (HF) group accommodating the remaining e^- in doubly occupied orbitals. VB orbitals describe the six π electrons of benzene, the electron of the incoming H atom, and the two σ electrons of the CH bond which is most distorted upon adsorption. Standard localization schemes have been employed to obtain the proper guess from HF orbitals. Wavefunction optimizations have been performed in the full spin space for nine electrons in a doublet state, whereas "diabatic" calculations have used the above optimized VB orbitals and constrained spin functions. See Ref. 50 for more details.]

B. Secondary adsorption

Next we consider adsorption of a second atom on the different sites $A(n)$ ($n=1, 6$) and $B(n)$ ($n=1, 6$) shown in Fig. 1, with a first adsorbed H atom on site A(0). For each site we have investigated the ground spin manifold by allowing full relaxation of the magnetization. In addition, in most of the cases, we have also performed magnetization-constrained calculations in order to get insights on both the singlet and the triplet states arising from the interaction between the doublet H-graphene ground-state and the second H atom.

The results for the binding energies are reported in Table II, along with the site-integrated magnetizations (M_{SI}) and the total magnetization M . Site-integrated spin densities have

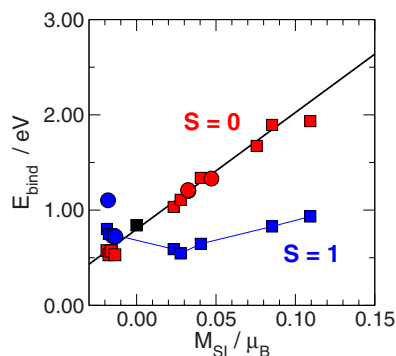


FIG. 6. (Color online) Binding energies for secondary H adsorption as a function of the site-integrated magnetization for singlet (red squares) and triplet (blue squares) states. Black square is the data point for single H adsorption. Also shown is a linear fit to the data set (solid line) and the H binding energy to form some four-atom clusters from three-atom ones (red and blue circles for final singlet and triplet states, respectively). See text for details.

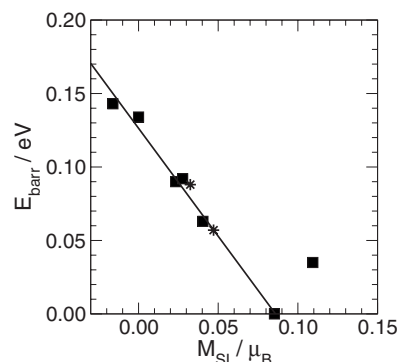


FIG. 7. Barrier energies for secondary atom adsorption as a function of the site-integrated magnetization. Linear regression (solid line) includes all data represented with squares, with the exception of the value of the *ortho* dimer (rightmost point in the graph). Data point at $M_{Si}=0$ is for single H adsorption; star is for forming a four-atom cluster from a three-atom one.

483 electrons are left in excess on the *B* sublattice, and they more
484 favorably couple at high spin.

485 The relationship between the available unpaired electron
486 density at a given site and the binding energy of adsorbing a
487 second H atom can be made clearer by reporting the energy
488 data of Table II as a function of M_{Si} . This is shown in Fig. 6,
489 for both the singlet and triplet states of the dimers, along
490 with the value for the first H adsorption (data point at M_{Si}
491 = 0). It is clear from the figure that with the exception of the
492 value for the *ortho* dimer [$A(0)B(1)$ in Fig. 1, this value has
493 been excluded from the linear regression shown in Fig. 6], a
494 linear relationship between the binding energy and the site-
495 integrated magnetization well describes the situation, and the
496 binding energy for single H adsorption fits well to this pic-
497 ture.

498 This is again consistent with the chemical model, as long
499 as the site-integrated magnetization is a measure of the un-
500 paired electron density available. According to Sec. III A,
501 adsorption of the first hydrogen atom arises from the energy
502 balance between a “localization energy” (the spin excitation
503 needed to set free an unpaired electron on the given lattice
504 site), the spin pairing forming the bond, and the surface re-
505 construction energy. The same is true for adsorption of a
506 second atom: localization energy takes only a slightly differ-
507 ent form than before because an unpaired electron is already
508 available in one of the two sublattices, but surface recon-
509 struction energy is not expected to depend on the adsorption
510 site. [In terms of the wavefunction of Eq. (1) this localization
511 energy can be defined by observing that the structures in
512 which the spin-up density localizes on the $(N-1)$ th site (N
513 even) correspond to $\Psi = A(\phi_1 \phi_2 \cdots \phi_{N-1} \Theta_{loc}^{N-1})$, where Θ_{loc}^{N-1} is
514 constrained to have the form $\Theta_{loc}^{N-1} = (c_1 \Theta_{0,0}^{N-2} + c_2 \Theta_{1,0}^{N-2}) \alpha$,
515 whereas the ground-state spin function comprises additional
516 contributions from $\Theta_{1,1}^{N-2} \beta$ structures.] Then, adsorption ener-
517 gies depend on the electronic properties only, and the linear
518 behavior observed for singlet-state dimers in Fig. 6 suggests
519 that the energy needed to localize the unpaired electron on a
520 given site decreases *linearly* when increasing the unpaired
521 electron density available. Notice that negative values of M_{Si}
522 (as found at *A* sites) correspond to a spin excess *parallel* to

that of the incoming H electron, and for these sites localiza- 523
tion of an unpaired electron with an *antiparallel* spin re- 524
quires increasingly more energy when the (magnitude of the) 525
spin density increases since this can only be achieved by 526
adding one electron to the site. On the other hand, when a 527
triplet dimer is formed upon adsorption the H electron does 528
not make use of the unpaired electron available, and adsorp- 529
tion energies are all around ~ 0.8 eV, i.e., of the order of the 530
first H adsorption. The effect of surface relaxation is only 531
seen in forming the *ortho* dimer, where few tenths of eV 532
more than the single H relaxation energy are required be- 533
cause of the closeness of the two hydrogen atoms. 534

Analogous linear behavior can be found when consider- 535
ing the computed energy barrier to sticking as a function of 536
the site-integrated magnetization, as shown in Fig. 7 for a 537
number of dimers (in their ground electronic state). This 538
agrees with the above localization energy and with the com- 539
mon tendency for a linear relationship between the binding 540
and the barrier energies for activated chemical reactions 541
(Brønsted–Evans–Polayni rule), the only exception being the 542
ortho dimer considered above. In agreement to previous theo- 543
retical studies we find that the *para* dimer [$A(0)B(2)$] shows 544
no barrier to adsorption, thereby supporting a preferential 545
sticking mechanism. This mechanism was first suggested by 546
Hornekær *et al.*³⁹ who looked at the STM images formed by 547 AQ:
exposing highly oriented pyrolytic graphite samples to a 548 #8
high-energy (1600–2000 K) H atom beam and observed forma- 549
tion of stable pairs, confirmed by first-principles 550
calculations.^{25,39} 551

We therefore find that formation of *AB* dimers is both 552
thermodynamically and kinetically favored over formation of 553
 A_2 dimers and single atom adsorption. This agrees with cur- 554
rent experimental observations which show evidence for 555
clustering of hydrogen atoms at all but very low ($<1\%$) 556
coverage conditions. In addition, we notice that the dimers 557
identified so far^{37–39} are all of the *AB* type. 558

C. Further adsorptions 559

We consider in this section results concerning formation 560
of clusters of three and four atoms. In these cases, the num- 561
ber of possible configurations is quite large and therefore we 562

TABLE III. Binding energies (E_{bind}) for addition of a third H atom to the *para* dimer structure $A(0)B(2)$ on the sites indicated in the first column (labels from Fig. 1).

Position	E_{bind} (eV)
A(2)	1.516
B(3)	0.847
A(3)	0.727
B(4) ($\equiv A(5)$)	0.971
A(4) ($\equiv B(6)$)	0.821
B(7)	0.727
B(8)	1.301

TABLE IV. Binding (E_{bind}) energies for adsorption to form H quadruples from the $A(0)B(2)B(8)$ cluster, along with the site-integrated magnetizations (M_{SI}) and the total ground-state magnetization (M), before and after adsorption, respectively. See Fig. 1 for atom labels.

	M_{SI} (μ_B)	E_{bind} (eV)	M (μ_B)
B(9)	-0.0180	1.103	2
A(7)	0.0471	1.331	0
B(6)	-0.0151	0.727	2
A(8)	0.0325	1.210	0
B(10)	-0.0134	0.723	2
A(9)	0.0326	1.201	0

limit our analysis to a few important cases. Following analogous notation recently introduced for defects by Palacios *et al.*,⁴⁸ we use the “chemical formula” A_nB_m to denote a cluster with n H atoms in the A lattice and m H atoms in the B lattice. According to Lieb’s theorem and to the π resonance picture, we expect that the ground electronic state has $|n - m|$ unpaired electrons. We have considered a number of A_2B_2 , A_2B , A_3B_1 , and A_3 clusters and found that their ground state has 0, 1, 2, and $3\mu_B$ of magnetization, respectively, in agreement with the expectation.

Three atom clusters have been obtained by adding one hydrogen atom either to a *para* dimer or to a *meta* dimer, i.e., $A(0)B(2)$ and $A(0)A(1)$ with the labels of Fig. 1, respectively. The binding energies of a third hydrogen atom to a *para* dimer structure are reported in Table III since they all are of A_2B type; the total magnetization for the resulting structures is $1\mu_B$. A look at Table III reveals that adsorption to a third hydrogen atom parallels that of the first H. This is consistent with the π resonance picture since AB dimers do not have unpaired electrons, and therefore show no preference toward any specific sublattice position. There are of course exceptions, notably the values for adsorption onto $A(2)$ and $B(8)$ lattice sites, and these can be reasonably ascribed to the effect of surface relaxation. Indeed, relaxation energies per atom in “compact” clusters may considerably differ from the value of the single H atom, being always of the order of the binding energies themselves (~ 0.8 eV). Similar conclusions hold when adding a third H atom to the (magnetic) *meta* dimer $A(0)A(1)$: adsorption on B lattice sites is strongly favored ($E_{\text{bind}}=1.2-1.9$ eV) and produces doublet structures ($M=1\mu_B$), whereas H atoms bind to A

lattice sites with an energy $\sim 0.7-0.8$ eV and produce highly magnetic structures ($M=3\mu_B$). Energy barriers to adsorption follow the same trend: preliminary calculations show that, with few exceptions, barriers to sticking a third H atom compare rather well with that for single H atom adsorption for the processes $AB \rightarrow A_2B$ and $A_2 \rightarrow A_3$ and may be considerably smaller for $A_2 \rightarrow A_2B$ ones.

In addition, again consistent with π resonance picture, we found that all the considered three-atom structures, with one or three unpaired electrons, show an alternation pattern in their spin-density maps. As an example, Fig. 8 reports the spin-density maps for an A_2B (left panel) and an A_3 (right panel) cluster. Analogous to Sec. III B we find that analysis of these spin-density maps gives insights to the adsorption properties of a fourth hydrogen atom. Table IV, for example, reports binding energies to form some four-atom clusters from the stable $A(0)B(2)B(8)$ one, the final total magnetization of the resulting structures and the values of the corresponding site-integrated magnetization before adsorption. The computed binding and barrier energies compare rather well with the dimer values, as can be seen in Figs. 6 and 7 where it is clear that the results fit well to the *same* linear trends obtained before. Few exceptions are for compact clusters where substrate relaxation does play some role. With such exceptions in mind, our results suggest that adsorption of hydrogen atoms on magnetic graphitic substrates (such as those obtained by adsorbing any odd number of H atoms), for a given final spin state, depends on the local spin density only.

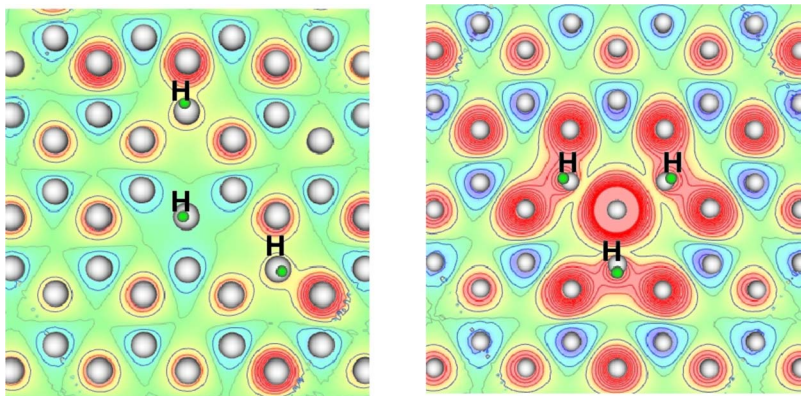


FIG. 8. (Color online) Spin density of 0.40 \AA above the surface for two three-atom clusters. Contour map with red/blue lines for spin-up/spin-down excess, respectively. Left and right panels for A_2B and A_3 clusters, respectively.

623 IV. SUMMARY AND CONCLUSIONS

624 In this work we have presented results of extensive first-
 625 principles calculations of the adsorption properties of hydro-
 626 gen atoms on graphite. A number of possible configurations
 627 involving one, two, three, and four atoms on the surface have
 628 been considered and barrier energies have been computed for
 629 some of them. We have found that adsorption of hydrogen
 630 atoms is strongly related to substrate electronic properties
 631 and used the chemical model of planar π conjugated systems
 632 to rationalize the data. The connection between this model
 633 and the valence theory of chemical bond on the one hand,
 634 and Hubbard models on the other hand, has been emphasized
 635 in Sec. III A and used at a qualitative level to rationalize our
 636 findings. In this way, one prominent feature of defective gra-
 637 phitic substrates, i.e., the possibility of forming ordered (mi-
 638 croscopic) magnetic patterns, turns out to be related to the
 639 spin alternation typical of π resonant systems. We have also
 640 invariably found in the cases considered that Lieb's theorem
 641 for repulsive Hubbard models can be used to predict spin
 642 alignment in ground-state graphitic structures.

643 Adsorption of single H atoms has been known for some
 644 time to be an activated process, with an energy barrier to
 645 sticking (we find ~ 0.14 eV) high enough to prevent adsorp-
 646 tion at ambient conditions. Adsorption of a second atom
 647 more favorably occurs on the $\sqrt{3} \times \sqrt{3}R30^\circ$ sublattice where
 648 spin density localizes and may proceed without barrier if it
 649 occurs on the so-called para site. This preferential sticking
 650 has been recently suggested by experimental and theoretical
 651 observations by Hornekær *et al.*^{38,39} We have extended the
 652 latter analysis by considering a large number of possible
 653 dimers and found that (i) binding (barrier) energies generally
 654 increase (decrease) linearly as a function of the site-
 655 integrated magnetization, and (ii) adsorption properties of
 656 the ortho site are slightly at variance with linear trends,
 657 thereby suggesting that substrate relaxation plays some role
 658 in this case.

659 When considering addition of a third atom we have
 660 found that the adsorption energetics of the incoming H atom
 661 is similar to that of the first one (i.e., a barrier ~ 0.15 eV
 662 high and a chemisorption well ~ 0.8 eV deep), unless we
 663 start with a "magnetic" dimer in which the two atoms are
 664 adsorbed in the same sublattice. (These structures, however,
 665 are kinetically and thermodynamically disfavored with re-
 666 spect to the unmagnetized AB configurations). This is in
 667 agreement with the chemical model, which predicts an
 668 "open-shell" configuration for A_2 dimers and a "closed-shell"
 669 one (with partial restoring of the π aromaticity) for AB ones.
 670 These results, therefore, suggest that preferential sticking due
 671 to barrierless adsorption is limited to formation of hydrogen
 672 pairs.

673 Finally, we have considered adsorption energetics in
 674 forming clusters of four atoms and regained the same picture
 675 obtained in forming pairs, namely, that adsorption is strongly
 676 biased toward the sublattice in which the spin density local-
 677 izes. Actually, the resulting energetics fits well to the linear
 678 behavior with respect to the site-integrated magnetization al-
 679 ready found for dimer formation. Such a linear relationship
 680 suggests that the energy needed to localize the unpaired elec-

tron on a given lattice site decreases linearly when increasing
 the site-integrated magnetization, at least in the range of val-
 ues covered by this study. Interestingly, this behavior sug-
 gests that if we were able to tune the magnetization of the
 substrate we could *control* the adsorption dynamics of H
 atoms.

Overall our results, consistent with the π resonance pic-
 ture, suggest that the *thermodynamically* and *kinetically* fa-
 vored structures are those that minimize sublattice imbal-
 ance, i.e., those $A_n B_m$ structures for which $n_l = |n - m|$ is
 minimum. The latter number n_l is also the number of midgap
 states in single-particle spectra which, according to the
 Hund-like rule provided by Lieb's theorem,⁹⁹ is directly re-
 lated to the total spin of the system, $S = n_l/2$, which is there-
 fore at minimum in the favored structures. Notice that how-
 ever small the S value can be, this result does not preclude
 the existence of local magnetic structures, antiferromagneti-
 cally coupled to each other. The case of an AB dimer with
 two atoms very far from each other provides such an ex-
 ample.

ACKNOWLEDGMENTS

The authors thank the NOTUR consortium and the
 CILEA computing center for providing computational re-
 sources. S.C. acknowledges the University of Oslo for the
 hospitality during his stay.

- ¹K. S. Novoselov, A. K. Geim, S. V. Morozov, D. Jiang, Y. Zhang, S. V. Dubonos, I. V. Grigorieva, and A. A. Firsov, *Science* **306**, 666 (2004). 706
- ²P. R. Wallace, *Phys. Rev.* **71**, 622 (1947). 707
- ³K. S. Novoselov, A. K. Geim, S. V. S. V. Morozov, D. Jiang, M. I. Katsnelson, I. V. Grigorieva, S. V. Dubonos, and A. A. Firsov, *Nature (London)* **438**, 197 (2005). 709
- ⁴Y. Zhang, Y.-W. Tan, H. L. Stormer, and P. Kim, *Nature (London)* **438**, 201 (2005). 712
- ⁵A. H. Castro Neto, F. Guinea, N. M. R. Peres, K. S. Novoselov, and A. K. Geim, arXiv:0709.1163v2 (2008). 714
- ⁶V. Mereghalli and M. Parrinello, *Appl. Phys. A: Mater. Sci. Process.* **72**, 143 (2001). 715 AQ: #9
- ⁷M. Mayer, V. Philipps, P. Wienhold, H. H. J. Seggern, and M. Rubel, *J. Nucl. Mater.* **290-293**, 381 (2001). 717
- ⁸L. Schlappbach and A. Züttel, *Nature (London)* **414**, 353 (2001). 718
- ⁹*The Molecular Astrophysics of Stars and Galaxies*, edited by T. W. Hartquist and D. A. Williams (Clarendon, Oxford, 1999). 719
- ¹⁰R. J. Gould and E. E. Salpeter, *Astrophys. J.* **138**, 393 (1963). 720
- ¹¹D. Hollenbach and E. E. Salpeter, *J. Chem. Phys.* **53**, 79 (1970). 721
- ¹²D. Hollenbach and E. E. Salpeter, *Astrophys. J.* **163**, 155 (1971). 722
- ¹³J. M. Greenberg, *Surf. Sci.* **500**, 793 (2002). 723 AQ: #10
- ¹⁴D. A. Williams and E. Herbst, *Surf. Sci.* **500**, 823 (2002). 724
- ¹⁵B. T. Draine, *Annu. Rev. Astron. Astrophys.* **41**, 241 (2003). 725
- ¹⁶L. Jeloica and V. Sidis, *Chem. Phys. Lett.* **300**, 157 (1999). 726
- ¹⁷X. Sha and B. Jackson, *Surf. Sci.* **496**, 318 (2002). 727
- ¹⁸X. Sha, B. Jackson, and D. Lemoine, *J. Chem. Phys.* **116**, 7158 (2002). 728
- ¹⁹T. Zecho, A. Güttler, X. Sha, B. Jackson, and J. Küppers, *J. Chem. Phys.* **117**, 8486 (2002). 729
- ²⁰X. Sha, B. Jackson, D. Lemoine, and B. Lepetit, *J. Chem. Phys.* **122**, 014709 (2005). 730
- ²¹S. Morisset, F. Aguillon, M. Sizun, and V. Sidis, *J. Chem. Phys.* **121**, 6493 (2004). 731
- ²²A. Allouche, Y. Ferro, T. Angot, C. Thomas, and J.-M. Layet, *J. Chem. Phys.* **123**, 124701 (2005). 732
- ²³S. Morisset, F. Aguillon, M. Sizun, and V. Sidis, *J. Chem. Phys.* **122**, 194702 (2005). 733
- ²⁴R. Martinazzo and G. F. Tantardini, *J. Phys. Chem. A* **109**, 9379 (2005). 734
- ²⁵N. Rougeau, D. Teillet-Billy, and V. Sidis, *Chem. Phys. Lett.* **431**, 135 (2006). 735
- ²⁶A. Allouche, A. Jelea, F. Marinelli, and Y. Ferro, *Phys. Scr., T* **T124**, 91 (2006). 736

- 746 (2006).
- 747 ²⁷J. Kerwin, X. Sha, and B. Jackson, *J. Phys. Chem. B* **110**, 18811 (2006).
- 748 ²⁸R. Martinazzo and G. F. Tantardini, *J. Chem. Phys.* **124**, 124702 (2006).
- 749 ²⁹R. Martinazzo and G. F. Tantardini, *J. Chem. Phys.* **124**, 124703 (2006).
- 750 ³⁰M. Bonfanti, R. Martinazzo, G. F. Tantardini, and A. Ponti, *J. Phys. Chem. C* **111**, 5825 (2007).
- 751 ³¹H. Cuppen and L. Hornekaer, *J. Chem. Phys.* **128**, 174707 (2008).
- 752 ³²T. Medina and B. Jackson, *J. Chem. Phys.* **128**, 114704 (2008).
- 753 ³³Y. Ferro, D. Teillet-Billy, N. Rougeau, S. Morisset, and A. Allouche, *Phys. Rev. B* **78**, 085417 (2008).
- 754 ³⁴A. Güttler, T. Zecho, and J. Küppers, *Chem. Phys. Lett.* **395**, 171 (2004).
- 755 ³⁵T. Zecho, A. Güttler, and J. Küppers, *Carbon* **42**, 609 (2004).
- 756 ³⁶A. Güttler, T. Zecho, and J. Küppers, *Surf. Sci.* **570**, 218 (2004).
- 757 ³⁷A. Andree, M. Le Lay, T. Zecho, and J. Küppers, *Chem. Phys. Lett.* **425**, 99 (2006).
- 758 ³⁸L. Hornekaer, Z. Sljivancanin, W. Xu, R. Otero, E. Rauls, I. Stensgaard, E. Laegsgaard, B. Hammer, and F. Besenbacher, *Phys. Rev. Lett.* **96**, 156104 (2006).
- 759 ³⁹L. Hornekaer, E. Rauls, W. Xu, Z. Sljivancanin, R. Otero, I. Stensgaard, E. Laegsgaard, B. Hammer, and F. Besenbacher, *Phys. Rev. Lett.* **97**, 186102 (2006).
- 760 ⁴⁰S. Baouche, G. Gamborg, V. V. Petrunin, A. C. Luntz, A. Bauricher, and L. Hornekaer, *J. Chem. Phys.* **125**, 084712 (2006).
- 761 ⁴¹S. C. Creighan, J. S. Perry, and S. D. Price, *J. Chem. Phys.* **124**, 114701 (2006).
- 762 ⁴²F. Islam, E. R. Latimer, and S. D. Price, *J. Chem. Phys.* **127**, 064701 (2007).
- 763 ⁴³L. Hornekaer, W. Xu, R. Otero, T. Zecho, E. Laegsgaard, and F. Besenbacher, *Chem. Phys. Lett.* **446**, 237 (2007).
- AQ: #11 774 ⁴⁴V. M. Pereira, F. Guinea, J. M. B. Lopes dos Santos, N. M. R. Peres, and A. H. Castro Neto, *Phys. Rev. Lett.* **96**, 036801 (2006).
- 775 ⁴⁵O. V. Yazyev and L. Helm, *Phys. Rev. B* **75**, 125408 (2007).
- 776 ⁴⁶L. Pisani, B. Montanari, and N. M. Harrison, *New J. Phys.* **10**, 033002 (2008).
- 777 ⁴⁷V. M. Pereira, J. M. B. Lopes dos Santos, and A. H. Castro Neto, *Phys. Rev. B* **77**, 115109 (2008).
- 778 ⁴⁸J. J. Palacios, J. Fernandez-Rossier, and L. Brey, *Phys. Rev. B* **77**, 195428 (2008).
- 779 ⁴⁹O. V. Yazyev, *Phys. Rev. Lett.* **101**, 037203 (2008).
- 780 ⁵⁰M. Bonfanti, R. Martinazzo, G. F. Tantardini, and A. Ponti (unpublished).
- 781 ⁵¹G. Kresse and J. Hafner, *Phys. Rev. B* **49**, 14251 (1994).
- 782 ⁵²G. Kresse and J. Hafner, *Phys. Rev. B* **47**, 558 (1993).
- 783 ⁵³G. Kresse and J. Furthmüller, *Comput. Mater. Sci.* **6**, 15 (1996).
- 784 ⁵⁴G. Kresse and J. Furthmüller, *Phys. Rev. B* **54**, 11169 (1996).
- 785 ⁵⁵P. E. Blochl, *Phys. Rev. B* **50**, 17953 (1994).
- 786 ⁵⁶G. Kresse and D. Joubert, *Phys. Rev. B* **59**, 1758 (1999).
- 787 ⁵⁷J. P. Perdew, K. Burke, and M. Ernzerhof, *Phys. Rev. Lett.* **77**, 3865 (1996).
- 788 ⁵⁸J. P. Perdew, K. Burke, and M. Ernzerhof, *Phys. Rev. Lett.* **78**, 1396 (1997).
- 789 ⁵⁹P. E. Blochl, O. Jepsen, and O. K. Andersen, *Phys. Rev. B* **49**, 16223 (1994).
- 790 ⁶⁰M. Hasegawa and K. Nishidate, *Phys. Rev. B* **70**, 205431 (2004).
- 791 ⁶¹H. Rydberg, N. Jacobsen, P. Hyldgaard, S. I. Simak, B. I. Lundqvist, and D. C. Langreth, *Surf. Sci.* **532–535**, 606 (2003).
- 792 ⁶²J. Kerwin and B. Jackson, *J. Chem. Phys.* **128**, 084702 (2008).
- 793 ⁶³Y. Ferro, F. Marinelli, and A. Allouche, *Chem. Phys. Lett.* **368**, 609 (2003).
- 794 ⁶⁴E. J. Duplock, M. Scheffler, and P. J. D. Lindan, *Phys. Rev. Lett.* **92**, 225502 (2004).
- 795 ⁶⁵T. Roman, W. A. Diño, H. Nakanishi, H. Kasai, T. Sugimoto, and K. Tange, *Carbon* **45**, 218 (2007).
- 796 ⁶⁶L. Chen, A. C. Cooper, G. P. Pez, and H. Cheng, *J. Phys. Chem. C* **111**, 18995 (2007).
- 797 ⁶⁷P. O. Lehtinen, A. S. Foster, Y. Ma, A. V. Krasheninnikov, and R. M. Nieminen, *Phys. Rev. Lett.* **93**, 187202 (2004).
- 798 ⁶⁸D. W. Boukhvalov, M. I. Katsnelson, and A. I. Lichtenstein, *Phys. Rev. B* **77**, 035427 (2008).
- 799 ⁶⁹M. Inui, S. A. Trugman, and E. Abrahams, *Phys. Rev. B* **49**, 3190 (1994).
- 800 ⁷⁰H. A. Mizes and J. S. Foster, *Science* **244**, 559 (1989).
- 801 ⁷¹P. Ruffieux, O. Groning, P. Schwaller, L. Schlapbach, and P. Groning, *Phys. Rev. Lett.* **84**, 4910 (2000).
- 802 ⁷²K. Kusakabe and M. Maruyama, *Phys. Rev. B* **67**, 092406 (2003).
- 803 ⁷³D. Jiang, B. G. Sumpter, and S. Dai, *J. Chem. Phys.* **127**, 124703 (2007).
- 804 ⁷⁴O. V. Yazyev, W. L. Wang, S. Meng, and E. Kaxiras, *Nano Lett.* **8**, 766 (2008).
- 805 ⁷⁵O. V. Yazyev and M. I. Katsnelson, *Phys. Rev. Lett.* **100**, 047209 (2008).
- 806 ⁷⁶L. Pauling and E. B. Wilson, *Introduction to Quantum Mechanics With Applications to Chemistry* (McGraw-Hill, New York, 1935).
- 807 ⁷⁷W. Heitler and F. London, *Z. Phys.* **44**, 455 (1927).
- 808 ⁷⁸G. F. Tantardini, M. Raimondi, and M. Simonetta, *Int. J. Quantum Chem.* **7**, 893 (1973).
- 809 ⁷⁹M. Raimondi, M. Simonetta, and G. F. Tantardini, *Comput. Phys. Rep.* **2**, 171 (1985).
- 810 ⁸⁰G. Rumer, *Gott. Nachr.* **■**, 377 (1932).
- 811 ⁸¹J. Gerratt, *Adv. At. Mol. Phys.* **7**, 141 (1971).
- 812 ⁸²D. L. Cooper, J. Gerratt, and M. Raimondi, *Chem. Rev. (Washington, D.C.)* **91**, 929 (1991).
- 813 ⁸³D. L. Cooper, *Valence Bond Theory*, Theoretical and Computational Chemistry Vol. 10 (Elsevier, Amsterdam, 2002).
- 814 ⁸⁴J. Li and R. McWeeny, *Int. J. Quantum Chem.* **89**, 208 (2002).
- 815 ⁸⁵G. F. Tantardini, M. Raimondi, and M. Simonetta, *J. Am. Chem. Soc.* **99**, 2913 (1977).
- 816 ⁸⁶D. L. Cooper, J. Gerratt, and M. Raimondi, *Nature (London)* **323**, 699 (1986).
- 817 ⁸⁷D. L. Cooper, J. Gerratt, and M. Raimondi, in *Ab Initio Methods in Quantum Chemistry II*, edited by K. P. Lawley (Wiley, New York, 1987).
- 818 ⁸⁸J. Hubbard, *Proc. R. Soc. London, Ser. A* **276**, 238 (1963).
- 819 ⁸⁹J. Wu, T. G. Schmalz, and D. J. Klein, *J. Chem. Phys.* **117**, 9977 (2002).
- 820 ⁹⁰J. Wu, T. G. Schmalz, and D. J. Klein, *J. Chem. Phys.* **119**, 11011 (2003).
- 821 ⁹¹R. Pariser and R. G. Parr, *J. Chem. Phys.* **21**, 466 (1953).
- 822 ⁹²R. Pariser and R. G. Parr, *J. Chem. Phys.* **21**, 767 (1953).
- 823 ⁹³J. A. Pople, *Trans. Faraday Soc.* **49**, 1375 (1953).
- 824 ⁹⁴A. Cresti, N. Nemec, B. Biel, G. Niebler, F. Triozon, G. Cuniberti, and S. Roche, *Nano Res* **1**, 361 (2008).
- 825 ⁹⁵J. Fernandez-Rossier, *Phys. Rev. B* **77**, 075430 (2008).
- 826 ⁹⁶J. Li and R. McWeeny, *SciNet Technologies Technical Report No.* **■**, 2007.
- 827 ⁹⁷J. Li and R. McWeeny, *Int. J. Quantum Chem.* **14**, 1347 (1993).
- 828 ⁹⁸M. Schmidt, K. Baldrige, J. Boatz, S. Elbert, M. Gordon, J. Jensen, S. Koseki, N. Matsunaga, K. Nguyen, S. Su *et al.*, *J. Comput. Chem.* **14**, 1347 (1993).
- 829 ⁹⁹R. McWeeny, *Adv. Quantum Chem.* **31**, 15 (1998).
- 830 ¹⁰⁰E. H. Lieb, *Phys. Rev. Lett.* **62**, 1201 (1989).

AUTHOR QUERIES — 017905JCP

- #1 Au: Please check our change from “=” to “denotes”.
- #2 Au: Please check our change from “Heitler, London, Pauling and Slater” to “Heitler and London(superscript 77) and Pauling and Slater”.
- #3 Au: Please check our change from “razionalizing” to “rationalizing”.
- #4 Au: Please check our change from “comma” to “and” after “processes”.
- #5 Au: Please check our change from “complementary” to “complementary”.
- #6 Au: Please verify our change from “..” to center dots in Eq. (1) and in succeeding equations.
- #7 Au: Please check our change from “the following sections” to “Secs. IIIB and IIIC”.
- #8 Au: Please spell out STM if possible.
- #9 Au: Please update Refs. 5 and 50.
- #10 CrossRef reports the author should be “MAYOGREENBERG” not “Greenberg” in the reference 13 “Greenberg, 2002”.
- #11 CrossRef reports the author should be “HORNEKAR” not “Hornekær” in the reference 43 “Hornekær, Xu, Otero, Zecho, Laegsgaard, Besenbacher, 2007”.
- #12 Au: Please supply the full journal title, CODEN, and/or ISSN and supply volume number in Ref. 80.
- #13 Au: References 84 and 97 contain the same information. Please check our deletion of Ref. 97 and renumbering of Refs. 97–99 throughout. There are now a total of 99 references instead of 100.
- #14 Au: Please supply the full journal title, CODEN, and/or ISSN in Ref. 94.
- #15 Au: Please supply report number in Ref. 96.
- #16 Au: Please supply all authors and verify deletion of “version March 24, 2007” in Ref. 97.
- #17 Au: Please be aware that although a caption makes reference to color online, figures in print will appear in black and white.